

Mass absorption coefficient of tungsten for 1600–2100 eV

Zachary H. Levine and Steven Grantham

National Institute of Standards and Technology, Gaithersburg, Maryland 20899-8410

Ian McNulty

Advanced Photon Source, Argonne National Laboratory, 9700 S. Cass Avenue, Argonne, Illinois 60439

(Received 5 June 2001; published 24 January 2002)

The transmission of soft x rays with photon energies from 1606 eV to 2106 eV was measured for tungsten using thin-film samples and a synchrotron source. This region includes the M_{IV} and M_V edges. The two tungsten films had thicknesses of 107.7 ± 10 nm and 51.5 ± 10 nm; the intensity of the transmitted x rays was measured with a silicon photodiode. The values for the mass absorption coefficient reported here were determined from the ratios of the transmission through the two samples, i.e., through a net 56.2 ± 14 nm of tungsten, and some additional constant factors. The $M_{V,IV}$ edges have widths (10%–90% after background subtraction) of 33 ± 5 eV and 28 ± 5 eV, respectively, compared to zero width in all x-ray tables based on atomic form factors and to 41 eV and 44 eV within a real-space multiple-scattering theory. The measurements are relevant to microspectroscopy and microtomography of integrated circuit interconnects and may be applicable to accurate measurement of the mass absorption coefficients of similar dense elements.

DOI: 10.1103/PhysRevB.65.064111

PACS number(s): 78.70.Dm, 34.50.Bw

I. INTRODUCTION

Recently, thicknesses of parts of an integrated circuit interconnect were measured using transmission coefficients obtained from scanning transmission x-ray microscopy¹ (STXM) and mass absorption coefficients from x-ray tables.² A similar study, comparing thickness information from transmission coefficients, atomic force microscopy, and tomography, was performed on a germanium test pattern with sub-micron features.³ STXM has also been used to obtain three-dimensional information on integrated circuit interconnects using tomography.^{4–6} For tomography to be efficient a transmission factor close to e^{-2} is desirable;⁷ for a sample of a given size and material, this indicates that the mass absorption coefficient should be in a certain parameter range. A suitable mass absorption coefficient can be selected only by adjusting the photon energy; hence, x-ray tables are a convenient tool for designing x-ray tomography experiments.

Chantler^{8,9} suggested that there is an uncertainty of up to a factor of 3 in the 1–3 keV region in the tabulated mass absorption coefficients, in contrast to the 5% uncertainty estimate also given recently¹⁰ and 30% quoted in Ref. 1. Energies just below the silicon K edge at 1839 eV were used in STXM studies of integrated circuit interconnects^{1,4–6} to achieve near-optimal penetration⁷ through several micrometers of silica. Among the materials commonly found in integrated circuit interconnects,¹¹ tungsten has two absorption features in this region, the M_V at 1809 eV and the M_{IV} at 1872 eV.² We were motivated to measure the M_V edge to improve the reliability of using x-ray transmission to obtain depth information as well as to understand the line shape to assess the prospects for using it for microspectroscopy of integrated circuit interconnect samples. We measured the M_{IV} edge, the spin-orbit split partner of the M_V as well.

The measurements presented here cover the spectral region continuously from 1606 to 2106 eV. Previous measurements of the mass absorption coefficient of tungsten in this

spectral region have been limited to the $K\alpha$ emission lines of Al and Si at 1487 and 1739 eV, respectively.^{12,13}

II. EXPERIMENT

Two thin films of tungsten were made by Luxel Corporation using ion-assisted deposition using 400 eV argon ions. The manufacturer reported a thickness of 107.7 ± 10 nm and 51.5 ± 10 nm for the two films, as measured by profilometry. (All uncertainties quoted herein are total with a 95% confidence interval.) The key parameter is the difference in thickness, 56.2 ± 14 nm. The samples were floated onto Lexan substrates of thickness 229.5 ± 20 nm and 222.5 ± 20 nm, respectively. The 7 ± 28 nm difference in the thickness of the substrates is neglected because Lexan is a polymer, and hence its attenuation length² ranges from 9 to 21 μm across 1606–2106 eV. The samples were held at room temperature in an aluminum box wrapped in a sealed plastic bag containing desiccant for 3.5 years before the x-ray measurements. The samples appeared uniform when inspected visually by microscope just prior.

The measurements were made at beamline 2-ID-B of the Advanced Photon Source (APS).¹⁴ The undulator beam is monochromatized by a water-cooled spherical grating monochromator with a constant deviation angle of 4.5° , a rhodium-coated grating with ion-etched laminar grooves, and adjustable entrance and exit slits. Harmonics of the undulator fundamental energy are effectively suppressed above 2.8 keV by two rhodium-coated mirrors operating in tandem at a grazing incidence angle of 1.25° . Including the diffraction efficiency of the grating, harmonic content is conservatively estimated to be below 1%. The incident photon energy was scanned from 2106 eV to 1606 eV in 5 eV steps and separately from 1906 eV to 1806 eV in 1 eV steps with 1 s observation time per data point. Both the samples and the photodiode were in air. Scans with the samples removed from the beam were also made. The x-ray beam had an an-

nular cross section with 98 μm outer diameter and 40 μm inner diameter. The flux transmitted by the sample was detected with an International Radiation Detectors Inc., AXUV-100-Ti2 absolute calibrated silicon photodiode with a 180 nm Ti filter. These photodiodes are known to have excellent response uniformity, very stable quantum efficiency, and NIST-traceable responsivity over the 100–4000 eV photon energy range.¹⁵ The monochromator resolution ranged from $\Delta E = 5.1$ eV at 2106 eV to $\Delta E = 3.0$ at 1606 eV; a second run was taken with $\Delta E = 8.6$ eV at 2106 eV, becoming $\Delta E = 5.0$ eV at 1606 eV, calculated for the beamline parameters with a method presented earlier.¹⁶

Although the thickness of the films was measured, the areal mass density has additional uncertainty. The bulk density of tungsten is 19.3 g/cm^3 . However, thin films may, in an unusual case, have a density as low as 0.5 times the bulk density.¹⁷ We take this factor to be 0.9 ± 0.1 , based on the experience of the vendor in making similar samples, leading to the value $\rho = 17.4 \pm 1.9$ g/cm^3 .

The raw photodiode current data was normalized by the current in the APS storage ring. Due to the presence of silicon in the beamline optics and the photodiode, a pronounced Si K edge was evident in the data. We added a constant value of 6 eV to the nominal calibration of the beamline monochromator to set the known position (1839 eV) of this edge. We relied on a calibration of the monochromator performed previously to set the energy scale.

We determine the transmission coefficient of the difference in thickness of the tungsten films from the formula

$$T = \frac{I_{\text{thick}}/I_{\text{ring-thick}}}{I_{\text{thin}}/I_{\text{ring-thin}}}$$

where I_{thick} is photodiode current with the thick sample in place and $I_{\text{ring-thick}}$ is the corresponding ring current (recorded separately for each 1 s interval); similar definitions hold for the thin sample. This method has the advantage of correcting for the beamline, air path, and detector efficiencies. The incident x-ray intensity was proportional to the ring current, which was nearly constant during our observation period. The only difference between thin and the thick samples was the *interior* tungsten in the thicker sample. The substrates were negligibly different, as argued above; moreover, the two materials had nearly identical surface properties (oxides, etc.), so the experiment was reasonably immune to surface effects. Also, there were no unexpected x-ray lines, which rules out contamination from 23 elements (Si, Se-Y, Sm-Ir). Gullikson and co-workers have made a similar argument for a related measurement.¹⁸ The reproducibility of the measurement is 10% in the worst case; this figure is taken as the uncertainty. Consistent with the literature, we present values for the mass absorption coefficient η [conventionally $[\mu/\rho]$ (Ref. 8)] in cm^2/g , taking the atomic weight of W to be 183.84 amu (1 amu = $1.660\,538\,73 \times 10^{-24}$ g). The mass absorption coefficient is determined from Beer's law

$$T = e^{-\eta t},$$

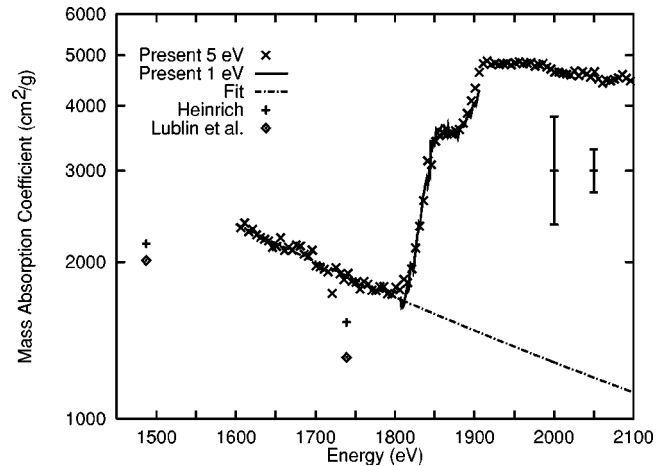


FIG. 1. Mass absorption coefficient, as measured in present experiment and from line source data [diamonds (Ref. 12) and + (Ref. 13)]. The larger error bar gives our uncertainty in the absolute value of our data within a 95% confidence interval; on the semilogarithmic plot, this uncertainty permits a rigid shift of the data. The smaller error bar denotes the relative uncertainty for the mass absorption coefficient at any given energy including both pointwise errors and drifts. Two runs are presented: using \times symbols for data taken with 5 eV spacing over the full range and using a solid line for data taken from 1806 to 1906 eV. The dash-dotted line is a power-law fit to the present data from 1606 to 1801 eV.

where ρ is the mass density and t is the sample thickness (or thickness difference in our case). Explicitly, $\eta = -(\ln T)/(\rho t)$. The figures below are presented on a semilogarithmic scale so that the reader may easily assess the affect of a constant factor (e.g., due to uncertainties in ρt) by a rigid shift. The quantity ρt has an uncertainty of $\pm 27\%$. Despite the dramatic change in the responsivity of the system at the silicon K edge, there is no hint of an artifact at this edge in the transmission coefficient data. We note that the small W fluorescence background which will have been present in the experiment posed a negligible contribution to these uncertainties, primarily due to the low yield of M fluorescence at these energies and the limited solid angle of our detector. In the following discussion, we consider only the data taken at the higher-energy resolution. The lower-resolution data were only used to estimate the uncertainty in the former, namely, $\pm 10\%$.

In Fig. 1, our data are compared to experimental mass absorption data on tungsten in this spectral region which we were able to find in the literature. Our value for the mass absorption coefficient is higher, agreeing within uncertainties with one experiment, but not the second.

III. COEFFICIENT BELOW THE ABSORPTION THRESHOLD

In the absence of an absorption threshold, the mass absorption coefficient η usually decreases with the photon energy E as $\eta(E) = \eta_0 E^{-\alpha}$ where η_0 is a material-specific constant and α , to a certain extent, a universal constant.¹⁹ The present data obey such a relationship, as shown in Figs. 1 and 2. An exponent may be derived from the two previous

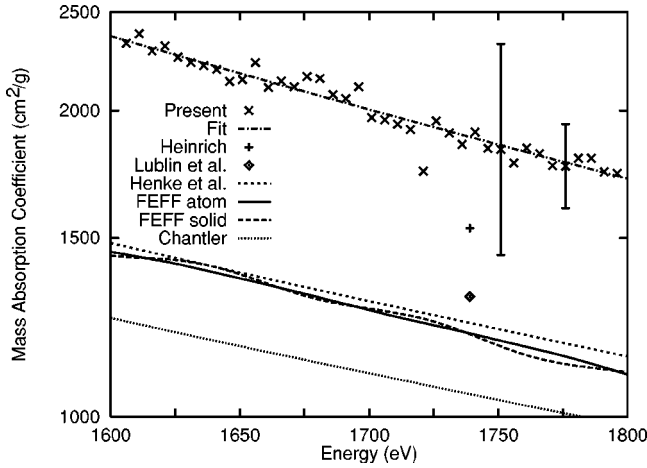


FIG. 2. Mass attenuation coefficient from present experiment (\times), line source data [diamonds (Ref. 12) and + (Ref. 13)], two comprehensive x-ray tables (short dashed line (Ref. 2) and dotted line (Ref. 9), and present FEFF calculation (Refs. 21 and 22) including all N shells within atomic (solid line) and solid-state (long dashed line) approximations. Error bars denote uncertainties as described in the caption to Fig. 1. The dot-dashed line is a power-law fit to the present data.

measurements; these values and the value of the exponent are given in Table I. The two values measured from line sources are in rough agreement and both are consistent with the present value within our uncertainty.

There have been several comprehensive tabulations of the x-ray spectra of many or all elements over broad spectral ranges.^{2,9,20} The subject has been reviewed recently with a 100-year perspective.¹⁰ The (relatively featureless) results are shown in Fig. 2. It may be seen that neither tabulation is in agreement with our measurements to within the joint uncertainty of the present measurement and the tables.

The mass absorption coefficient is dominated by photoelectric absorption, with corrections for W in this energy regime being well below 1%.⁹ Accordingly, it is appropriate to compare the measured data to calculations of the photoelectric cross section. We have performed a calculation using a popular real-space multiple-scattering model FEFF 8.10,^{21,22} which was developed as a tool for the analysis of x-ray absorption fine structure. Nevertheless, the code produces absolute values for cross sections, which are shown below threshold in Fig. 2 (after division by the atomic mass of W). The calculation includes all seven N shells; O shells are omitted. (A calculation we performed within the relativistic time-dependent local density approximation²³ indicates that this is a 5% approximation.) Again, the calculated values are well below the present measured values. The small predicted x-ray absorption fine structure is less than our experimental uncertainty.

We also performed an atomic calculation with the relativistic time-dependent local density approximation (RTDLDA), with and without dielectric screening. Some of the parameters are given in Table I; agreement with the present experiment is quite good. However, the RTDLDA cross section is too small both above and below threshold by about a factor of 2.

TABLE I. Two parameters related to the mass absorption coefficient of W: the exponent α relating the mass absorption coefficient and the energy via $\eta = E^{-\alpha}$ below the threshold and jump ratio τ of the M_{IV} contribution to the M_{IV} contribution of the mass absorption coefficient of W. “General values” refers to averages over many elements from experiments performed in the early days of quantum mechanics. “Statistical ratio” is the ratio of the number of electrons in the $3d_{5/2}$ and $3d_{3/2}$ orbitals. The symbols ΔE_{M_V} and $\Delta E_{M_{IV}}$ refer to the energy difference between the 10% and 90% values in the transition. IPA is the independent particle approximation and RTDLDA includes screening of the external x ray with the relativistic time-dependent local density approximation.

	α	τ	ΔE_{M_V}	$\Delta E_{M_{IV}}$
Table ^a	2.17	1.49	0	0
Table ^b	2.10	1.58	0	0
Expt. ^c	2.74			
Expt. ^d	2.23			
Present IPA ^e	2.07	1.73	37	32
Present RTDLDA ^e	2.58	1.36	36	35
Present FEFF ^f	2.36	1.57	41	44
Present expt.	2.74 ± 0.81	1.30 ± 0.30	33 ± 5	28 ± 5
General values ^g	2.5–3			
Statistical ratio		1.5		

^aReference 2.

^bReference 9.

^cReference 12.

^dReference 13.

^eReference 23.

^fReference 21 and 22.

^gReference 19.

IV. COEFFICIENT ABOVE THE ABSORPTION THRESHOLD

The transition widths are presented in Table I. The FEFF calculation and both variants of the RTDLDA calculation give a reasonable account of the transition widths. To ensure numerical accuracy, the FEFF results were calculated using full multiple scattering²¹ within 100 eV of each threshold. From the early days of quantum mechanics, it has been traditional to consider transitions at x-ray edges to be abrupt^{19,24} although it has also been known from that period that the transitions are continuous if resolved on a fine enough energy scale.¹⁹ Abrupt x-ray transitions are a feature of all x-ray tabulations of which we are aware.^{2,9,20,25} The models have a zero width for x-ray transitions which arises within the Dirac-Fock atomic model.⁹ A zero width is not necessarily a feature of atomic theory as exemplified by the relativistic time-dependent local density approximation.²³ In contrast, FEFF begins with an embedded-atom model which includes contributions from the potentials of the neighboring atoms.²⁶

To focus on the $M_{V,IV}$ edges, we opt to present all theory and measurements above threshold with the background from lower-energy transitions subtracted (our data and the tables^{2,9}) or omitted (FEFF calculations), as appropriate. The subtraction follows the power law formula discussed above and in Table I; see also Fig. 1. The results, along with a calculation performed by us using the FEFF 8.10 code, are shown in Fig. 3. The results of Refs. 2 and 9 are almost identical on this plot, so only one is presented. The tables

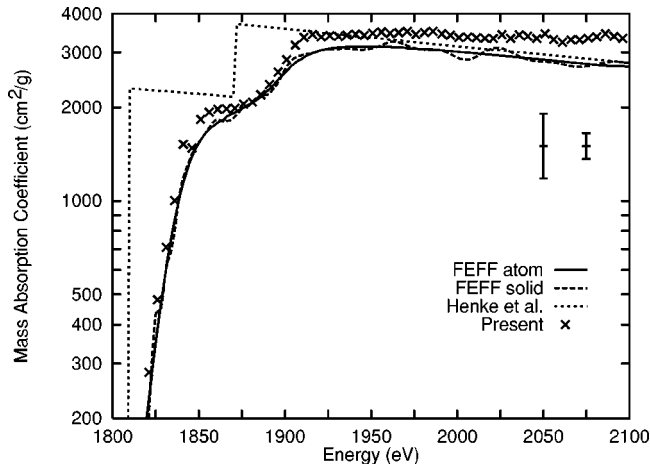


FIG. 3. Mass attenuation coefficient attributable to M -shell emission, from present experiment (\times) and an x-ray table [short dashed line (Ref. 2)] after subtraction of power-law background, and present FEFF calculation (Refs. 21 and 22) including only the $M_{IV,V}$ shells within atomic (solid line) and solid-state (long dashed line) approximations. The FEFF calculation is performed within its x-ray appearance near-edge structure (XANES) version within 100 eV of the M_{IV} and M_V edges. The results of Ref. 9 are almost identical to those of Ref. 2 and so are omitted here.

and the present experiment are in agreement within the uncertainties after the transition is completed; they differ radically for the widths. The tables caution that they are not valid near transition edges, particularly since solid-state effects are stronger there. The data are also in agreement with the results of the FEFF model within the experimental uncertainties, although at higher energies a possible discrepancy is emerging. On the experimental side, this may be due either to inaccurate background subtraction below the threshold or to a measurement error in the high-energy region. The fine structure is too small to be observed with our uncertainties. As remarked before, the RTDLDA model (not plotted) leads to values about a factor of 2 too low.

Also shown in Table I is the jump ratio τ of the M_V to M_{IV} transitions, using peak to trough values for the experiment and theories which yield a finite width. If one assumes that the only effect of spin-orbit splitting is to divide the electrons into two otherwise identical groups, the statistical ratio $6/4$ will prevail for this quantity. We are not able to distinguish between the theories and tables by this parameter, other than to note the screening of the RTDLDA brings the jump ratio τ into better agreement with the data.

V. CONCLUSIONS

The mass absorption ratio of tungsten thin films was measured over the energy range 1606–2106 eV using synchrotron radiation. Two samples were used to minimize the effect of the substrate, the sample surface and systematic factors due to the x-ray source, beamline, and detector. The results have been compared to data from x-ray tube sources, to x-ray tables, and to calculations within the models of FEFF and the RTDLDA. The transition has a finite width, which is pre-

dicted by the embedded atom model of FEFF as well as the purely atomic model of RTDLDA. It is not predicted by the zero-width Dirac-Fock approximation. Indeed, above threshold, FEFF gives an excellent account of the data in this regime. To understand the origin of the widths we argue that the transition is broad because the lowest-level unoccupied states in metallic tungsten have $5d$ character; transitions from a $3d$ state are dipole forbidden at threshold. At somewhat higher energies the virtual $5f$ orbitals yield a high density of states with dipole-allowed transitions.

We suggest, cautiously, that the success of the FEFF model within effective medium theory²⁷ may be suitable for the construction of tables. For a given atom, there is a particular density of the electron gas which minimizes that energy. In practice, this density is realized in real compounds, at least for the case of metallic alloys.²⁸ Hence, for condensed-matter applications the assumption that an atom is embedded in an electron gas whose density is an energetic minimum may be a better assumption for universal application than the assumption of a free atom.

For energies below the M_V edge, all theories and tables give values which are substantially lower than those obtained in all published experiments, especially the present one. Although the tables do not claim to be accurate just above absorption edges, they do claim accuracy below them. Yet the tables are not in agreement with the published experimental data in this regime. It is not entirely clear how to remedy this problem. The RTDLDA calculation suggests that dynamic screening effects are significant if agreement well below the factor-of-2 level is desired.

We were brought to the question of the mass absorption coefficient near the tungsten M_V edge from an attempt to understand two-dimensional (2D) and 3D x-ray images of integrated circuit interconnects. In particular, it would be desirable to quantify tungsten in samples using x-ray energies below the silicon K edge at 1839 eV. This may, in fact, be possible: for example, we measure the ratio of the tungsten mass absorption coefficient at 1830 eV to its value of 1810 eV to be 1.44 ± 0.20 ; since nearly all other elements will have a ratio just below unity for this parameter, imaging at these two energies may yield images with reasonable, although not ideal, contrast.

The results of this study are likely to find broader applications to other technologies depending on W thin films and accurate determination of the mass absorption coefficients of neighboring elements such as tantalum.

ACKNOWLEDGMENTS

The authors acknowledge useful discussions with Glen Lefeverbotton, Thomas Lucatorto, Charles Tarrío, and Robert Vest. Technical assistance from Sean Frigo and Timothy Mooney in support of the 2-ID-B beamline is also appreciated as well as assistance from Charles Bouldin and John Rehr regarding the FEFF code. The authors acknowledge funding provided by the Department of Energy, Basic Energy Sciences, Office of Energy Research, under Contract No. W-31-109-ENG-38.

- ¹X. Su, C. Stagarescu, G. Xu, D.E. Eastman, I. McNulty, S.P. Frigo, Y. Wang, C.C. Retsch, I.C. Noyan, and C.-K. Hu, *Appl. Phys. Lett.* **77**, 3465 (2000).
- ²B. Henke, E. Gullikson, and J. Davis, *At. Data Nucl. Data Tables* **54**, 181 (1993), http://www-cxro.lbl.gov/optical_constants/atten2.html
- ³A.R. Kalukin, B. Winn, Y. Wang, C. Jacobsen, Z.H. Levine, and J. Fu, *J. Res. Natl. Inst. Stand. Technol.* **275**, 867 (2000).
- ⁴Z.H. Levine, A.R. Kalukin, S.P. Frigo, I. McNulty, and M. Kuhn, *Appl. Phys. Lett.* **74**, 150 (1999).
- ⁵Z.H. Levine, A.R. Kalukin, M. Kuhn, S.P. Frigo, I. McNulty, C.C. Retsch, Y. Wang, U. Arp, T.B. Lucatoro, B.D. Ravel, and C. Tarrío, *J. Appl. Phys.* **87**, 4483 (2000).
- ⁶Z.H. Levine, S. Grantham, S. Neogi, S.P. Frigo, I. McNulty, C.C. Retsch, Y. Wang, and T.B. Lucatoro, *J. Appl. Phys.* **90**, 556 (2001).
- ⁷B.P. Flannery, H.W. Deckman, W.G. Roberge, and K.L. D'Amico, *Science* **237**, 1439 (1987).
- ⁸C.T. Chantler, *Radiat. Phys. Chem.* **13**, 231 (1999).
- ⁹C.T. Chantler, *J. Phys. Chem. Ref. Data* **29**, 597 (2000).
- ¹⁰J.H. Hubbell, *X-Ray Spectrom.* **28**, 215 (1999).
- ¹¹G.K. Rao, *Multilevel Interconnect Technology* (McGraw-Hill, New York, 1993).
- ¹²P. Lublin, P. Cukor, and R.J. Jaworowski, *Adv. X-Ray Anal.* **13**, 632 (1970).
- ¹³K.F.J. Heinrich, *X-Ray Absorption Uncertainty — The Electron Microprobe* (Wiley, New York, 1966), p. 296.
- ¹⁴I. McNulty, A.M. Khounsary, Y.P. Feng, Y. Qian, J. Barraza, C. Benson, and D. Shu, *Rev. Sci. Instrum.* **67**, 3372 (1996), CD-ROM.
- ¹⁵E.M. Gullikson, R. Korde, L.R. Canfield, and R.E. Vest, *J. Electron Spectrosc. Relat. Phenom.* **80**, 313 (1996).
- ¹⁶I. McNulty, Y.P. Feng, S.P. Frigo, and T.M. Mooney, *Proc. SPIE* **3150**, 195 (1997).
- ¹⁷L.I. Maissel and M.H. Francombe, *An Introduction to Thin Films* (Gordon and Breach, New York, 1973), pp. 117–118.
- ¹⁸E.M. Gullikson, P. Denham, S. Mrowka, and J.H. Underwood, *Phys. Rev. B* **49**, 16283 (1994).
- ¹⁹A.H. Compton and S.K. Allison, *X-Rays in Theory and Experiment*, 2nd ed. (Van Nostrand, Princeton, 1935), Sec. VII.6-8.
- ²⁰D.E. Cullen, J.H. Hubbell, and L. Kissel, Lawrence Livermore National Laboratory Report UCRL 50400 (Lawrence Livermore National Laboratory, Livermore, CA, 1997), Rev. 5, available in program form only.
- ²¹A.L. Ankudinov, B. Ravel, J.J. Rehr, and S.D. Conradson, *Phys. Rev. B* **58**, 7565 (1998).
- ²²A.L. Ankudinov and J.J. Rehr, *Phys. Rev. B* **62**, 2437 (2000).
- ²³D.A. Liberman and A. Zangwill, *Comput. Phys. Commun.* **32**, 75 (1984).
- ²⁴H.A. Bethe and E.E. Salpeter, *Quantum Mechanics of One- and Two-Electron Atoms* (Plenum, New York, 1957), Sec. 71.
- ²⁵W.J. Veigele, *At. Data* **5**, 51 (1973).
- ²⁶J.J. Rehr, C.H. Booth, F. Bridges, and S.I. Zabinsky, *Phys. Rev. B* **49**, 12347 (1994).
- ²⁷J.K. Nørskov and N.D. Lang, *Phys. Rev. B* **21**, 2131 (1980).
- ²⁸A. Zangwill and A.C. Redfield, *J. Phys. F* **18**, 1 (1988).